CO2 solubility measurements in brine under reservoir conditions

CO_2 Solubility Measurements in Brine under Reservoir Conditions: A Comparison of Experimental and Geochemical Modelling Methods

Luc Steel, Qi Liu, Eric Mackay and Mercedes Maroto-Valer, Heriot-Watt University, UK

Abstract: The dissolution of CO_2 in brine (solubility trapping) is one of the most secure and permanent trapping mechanisms when considering CO_2 geological storage. In addition, CO_2 dissolution in brine is an important mechanism of CO_2 enhanced oil recovery as it improves sweep efficiency and increases oil displacement. Currently, there is a range of experimental methods that have been used to measure CO_2 solubility in brine and a critical review of these methods is presented here. Several different geochemical models that can be used to calculate CO_2 solubility in brine are also reviewed and the importance of selecting the correct equation of state (EoS) is addressed. Furthermore, the validity of the experimental results was ascertained through a comparison of the published experimental results with those produced through geochemical modeling. The geochemical modeling software, HydraFLASH, can be used to accurately calculate CO_2 solubilities under a number of conditions provided the correct EoS is selected. For the purpose of CO_2-water systems, the Valderrama-Patel-Teja EoS is the most accurate as it is designed to be used for systems containing polar and non-polar compounds. By comparing the experimental results with those obtained through the geochemical modeling, it is concluded that the experimental procedure developed by Tong et al. (2013) is the most accurate means of measuring CO_2 solubility.

Keywords: CO_2 Enhanced Oil Recovery, CO_2 Geological Storage, CO_2 Solubility

1 Introduction

The International Energy Agency (IEA) has predicted that global total primary energy supply will rise to an estimated 16,500 Mtoe (Million tonne of oil equivalent) by 2030 with fossil fuels accounting for 75% of this value (approximately 12,500 Mtoe), while in 2012 fossil fuels accounted for roughly 10,900 Mtoe. [1,2] Consequently, global reliance on fossil fuels is only likely to increase over the next few decades. This presents two significant issues. The first being that fossil fuels are not an infinite resource and so increased reliance on fossil fuels will put major strain on reserves. Furthermore, increased burning of fossil fuels will result in higher CO_2 emissions which were already at a record high in 2014 with global annual CO_2 production levels of approximately 40Gt. [3] Therefore, strategies need to be employed to increase fossil fuel reserves and reduce CO_2 emissions. Two such strategies are Enhanced Oil Recovery (EOR) and Carbon Dioxide Capture and Storage (CCS).

The CO_2-EOR process involves injecting supercritical CO_2 into the reservoir, where it comes into contact with oil and may become miscible with the oil. [4] The CO_2 that dissolves in the oil causes it to swell, forming a concentrated oil bank which is then pushed towards the production well, allowing the oil to be extracted. CO_2-EOR is one of the most successful EOR technologies and will contribute to increasing the lifetime of fossil fuels reservoirs. However, although increasing fossil fuel reserves is vital to sustaining global energy demands in the future, increased burning of these fuels will result in more CO_2 emissions which need to be appropriately dealt with. It is for this reason that CCS technologies are necessary.

The first stage of CCS involves removing CO_2 from a flue gas through pre-, post- or oxyfuel-combustion. [5] Once the CO_2 has been captured it needs to be stored in a safe and permanent manner. At present, CO_2 storage within depleted oil and gas fields or deep saline aquifers is considered the preeminent means of storing CO_2. This is due to their large storage capacities

and the fact that some of the infrastructure needed for CO_2 injection is already in place as a result of the oil and gas industry. [6] Global storage capacities for CO_2 are expected to be in the range of 1,000-10,000Gt for deep saline aquifers and 920Gt for depleted oil and gas fields. [7] Comparing these values with global annual CO_2 emissions in 2014 of 40Gt, it is clear that these storage options have the potential to significantly reduce CO_2 emissions to the atmosphere.

There are two main purposes of this paper. The first is to provide an updated review of the experimental work that has been performed over recent years, in regard to measuring CO_2 solubility in brine. The corresponding sections will look at how the experimental methods have evolved and how the associated changes in technique and equipment have resulted in more accurate measurements. The second purpose is to assess some of the geochemical modelling software's that are available to calculate CO_2 solubility in brine, and to emphasise the importance of selecting the correct equation of state (EoS), which has not yet been discussed in previous literature. This EoS, along with the associated geochemical modelling software, will then be used to ascertain the validity of the published experimental results and confirm whether the accuracy of CO_2 solubility measurements has improved over recent years.

2 CO_2 Solubility in Brine

Upon injection into deep geological formations, such as depleted oil and gas fields and saline aquifers, CO_2 can be trapped through either physical or geochemical trapping mechanisms. [8] Physical trapping mechanisms include static (structural and stratigraphic), hydrodynamic and residual gas trapping. It is these mechanisms that initially trap CO_2 upon injection as geochemical trapping mechanisms take considerable time to come into play. [9] However, geochemical trapping results in the more permanent and secure storage of CO_2 and

is hence preferable to physical trapping. The two types of geochemical trapping are solubility and mineral trapping.

Solubility trapping involves CO_2 dissolving in the local brine and becoming trapped as an aqueous component (Eqn. 1). [10] The aqueous CO_2 then reacts with water to form carbonic species. The concentration of each of the three carbonic species, H_2CO_3, HCO_3^- and CO_3^{2-}, is dependent on the brine pH. H_2CO_3 (Eqn. 2) is the primary species at low pH (~4), HCO_3^- (Eqn. 3) dominates at the near neutral (~6) and at basic pH (~9), it is the CO_3^{2-} species (Eqn. 4) which are prevalent.

$$CO_2(g) \leftrightarrow CO_2(aq) \quad (1)$$

$$CO_2(aq) + H_2O \leftrightarrow H_2CO_3 \quad (2)$$

$$H_2CO_3 \leftrightarrow H^+ + HCO_3^- \quad (3)$$

$$HCO_3^- \leftrightarrow H^+ + CO_3^{2-} \quad (4)$$

After solubility trapping, the CO_2 is no longer in a separate phase and so the CO_2 fluid is not subject to the buoyant forces that drive it upwards. [11] The reason the CO_2 is no longer subject to buoyant forces is because CO_2 saturated brine is denser than unsaturated brine. Consequently, the CO_2 is now securely stored within the geological formation. CO_2 solubility in brine is not only fundamental to solubility trapping but it also affects CO_2-EOR. When CO_2 dissolves in brine, the sweep efficiency improves, and the CO_2 may still partition into and mobilise residually trapped oil contacted by the CO_2 saturated brine, and therefore, increase oil displacement.

2.1 Factors Affecting CO_2 Solubility

CO_2 solubility in brine is dependent on a number of factors, such as pressure, temperature, and salinity. [12] Figures 1-3 show both modelling and experimental data for CO_2 solubility under pressure, temperature and salinity conditions for CO_2 storage.

Figure 1 shows how CO_2 solubility in brine increases with pressure at a constant temperature of 323K and brine salinity of 1 mol NaCl/kg brine. This is explained by Henry's law which states that the concentration of dissolved gas at equilibrium is directly proportional to the partial pressure of the gas. [13] The open diamonds are the results of modelling achieved using a CO_2 solubility calculator created by Duan and Sun (2003) and Duan et al. (2006), whereas the black squares are experimental measurements by Nighswander et al (1989), Li et al. (2004) and Kiepe et al. (2002). [14,15,16,17,18] The experimental results are not consistent with one another due to different experimental procedures being employed in each case. A critical review of the different experimental procedures that can be used to measure CO_2 solubility is presented in Section 3.

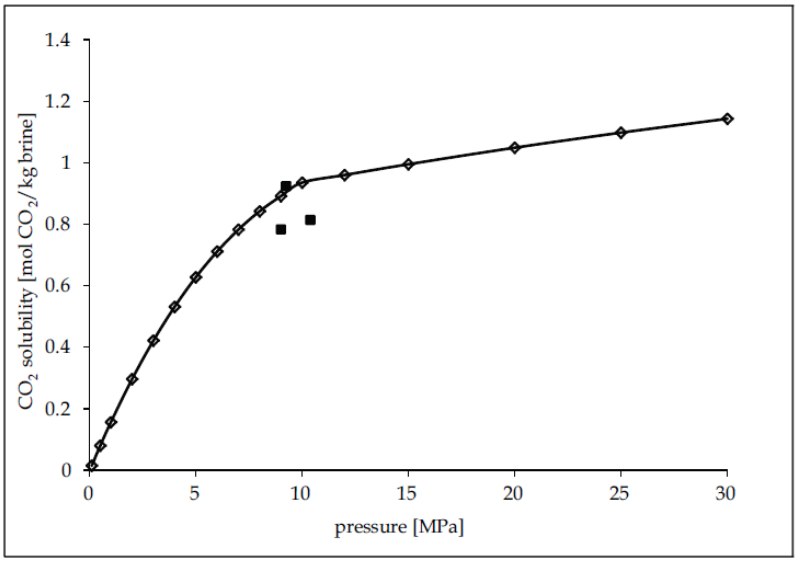

Figure 1: CO_2 solubility as a function of pressure at 323K and 1 mol NaCl/kg brine. Modelling and experimental data [12]

An increase in temperature has the opposite effect on brine solubility, as can be seen from Figure 2. When heat is added to a solution, the additional thermal energy is sufficient enough to overcome the attractive forces that exist between the solvent and the gas molecules. [13] This leads to a reduction in gas solubility and is why CO_2 solubility in water decreases with increasing temperature. Since temperature has a lesser effect on solubility than pressure, deep host rocks (800-1000m) are suitable for CO_2 storage, as the associated high pressures compensate for the increased temperatures. [6] In this case, the pressure was set to 10MPa and the salinity was once again 1 mol NaCl/kg brine. [12] As before, the modelling data is represented by the open diamonds, whereas the rest of the symbols correspond to the experimental measurements. It should be noted that the measurement by Rumpf et al. (1994) is significantly lower due to the experiment being run at high brine salinity. [19]

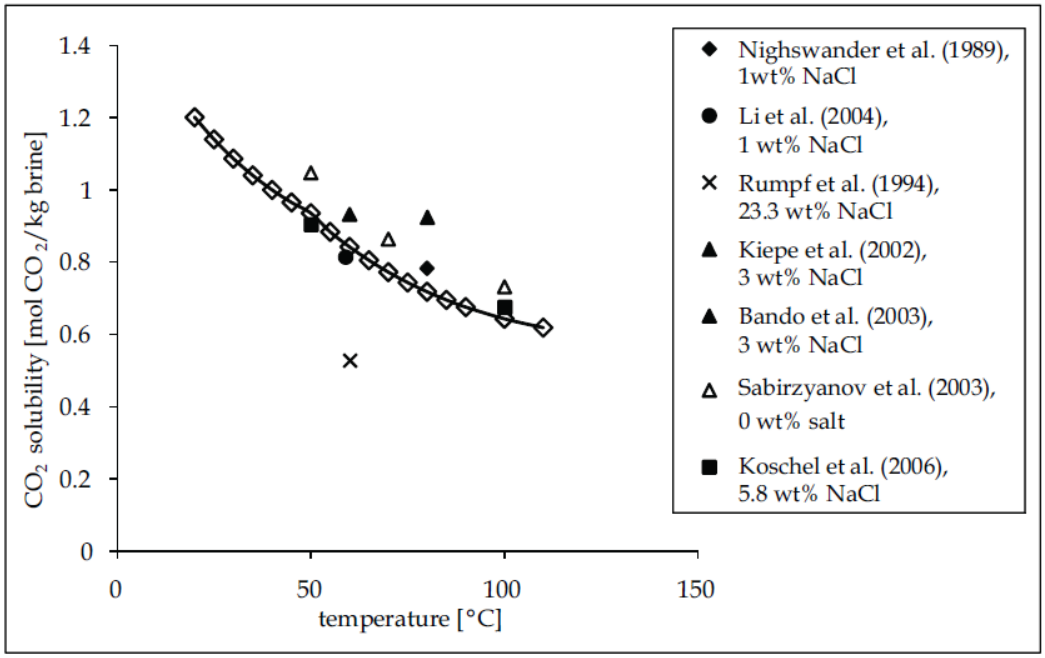

Figure 2: CO_2 solubility as a function of temperature at 10MPa and 1 mol NaCl/kg brine. Modelling and experimental data [12]

The results in Figure 3 show that, as with temperature, CO_2 solubility in brine decreases with increased brine salinity. This is a result of the salting out effect, where water can dissolve less

gas due to the presence of electrolytes. [20] This is due to the water molecules being attracted to the salt ions, which reduces the number of H^+ and O^{2-} ions that can capture and disassociate gas molecules. The pressure and temperature conditions were set to 10MPa and 323K, respectively. As with both previous data sets, the modelling results are shown as open diamonds with the rest of the symbols representing experimental measurements. It is unclear why the results from Sabirzyanov et al. (2003) and Dodds et al. (1956) are included since both sets of experiments were run at 0 wt% NaCl. Although the modelling data agrees with the experimental results, in terms of CO_2 solubility decreasing with increasing brine salinity, the CO_2 solubility calculator appears to over predict the CO_2 solubility in brine.

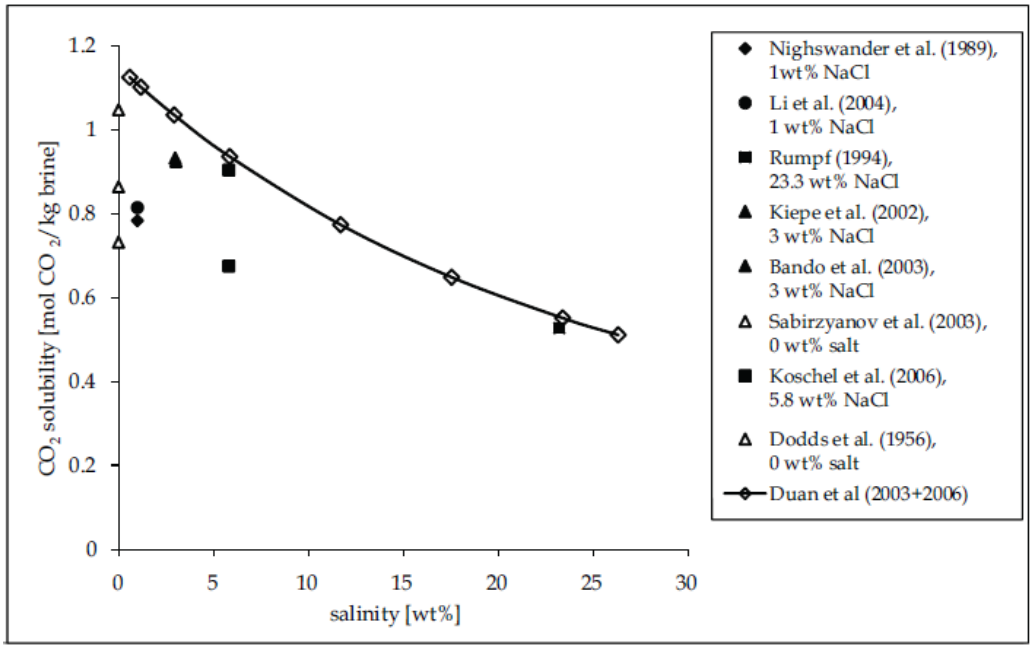

Figure 3: CO_2 solubility as a function of salinity at 323K and 10MPa. Modelling and experimental data [12]

The reason for the over prediction by the CO_2 solubility calculator and the large variation in results between the experimental data sets is a consequence of the difficulties of accurately measuring CO_2 solubility under reservoir conditions. These difficulties arise from the fact that much of the solubility measuring equipment cannot be used at reservoir pressures. As a result, in most cases the system has to be depressurised first, to atmospheric pressure, before

measurements can be taken. [21] Depressurising the system will result in CO_2 bubbling out of the brine and so an accurate measurement of CO_2 solubility cannot be made. This is why the results from the different experimental data sets, shown in the Figures 1-3, are not consistent even under the same conditions. [12]

3 Experimental Work

Over the past decade, there has been much experimental work trying to accurately measure CO_2 solubility under reservoir conditions with varying levels of success. This section reviews this work in detail and Table 1 provides a summary of the different experimental procedures that are discussed here.

Table 1: Summary of experimental procedures and how they compare

Main Component of Apparatus	**CO_2 Solubility Measured:**	**Reference**
High Pressure Cell	Titration	Rochelle et al. (2002)
High Pressure Cell	Mass and pressure of cylinder	Bando et al. (2003)
PVT Cell	Volume of evolved gas and mass of solution	Li et al. (2004)
PVT Cell	Adding CO_2(g) in cylinder + CO_2(g) released from cylinder + CO_2(aq) remaining in cylinder	Yan et al. (2011)
Autoclave Cell	Volume of evolved gas and mass of solution	Sabirzyanov et al. (2003)
Autoclave Cell	Coulometric Titration	Qin et al. (2008)
Autoclave Cell	Bubble point observation and masses of CO_2 and brine present	Tong et al. (2013)

3.1 CO_2 Solubility in Pure Water and Synthetic Utsira Porewater

In 2002, the British Geological Survey released a commissioned report on the solubility of supercritical CO_2 into pure water and synthetic Utsira porewater. [22] One of the aims of the report was to understand how much of the CO_2 injected into the Utsira formation would dissolve in the formation water. As a result, it was necessary to measure CO_2 solubility under

reservoir conditions. To try and achieve this, CO_2 (at a known pressure and fixed temperature) was injected into a vessel containing brine and CO_2 in its aqueous phase was taken under experimental pressure, but at room temperature. The experimental apparatus used for this work is shown in Figure 4 and consisted of a CO_2 cylinder which was connected to a syringe pump that could rapidly increase the gas pressure to supercritical conditions. The supercritical CO_2 was then injected into a stainless steel pressure vessel which contained either pure water or synthetic Utsira porewater, depending on the experiment taking place. The pressure vessel was contained within an oven to keep the temperature constant and a magnetic stirrer was used to promote dissolution of the gas. The sampling of the aqueous CO_2 was achieved via a dip tube that ensured that only the aqueous phase was sampled. When the sample was taken, it was cooled to room temperature which increased the CO_2 solubility (as solubility increases with decreasing temperature) and also reduced the chance of degassing as the aqueous solution was below the CO_2 saturation point.

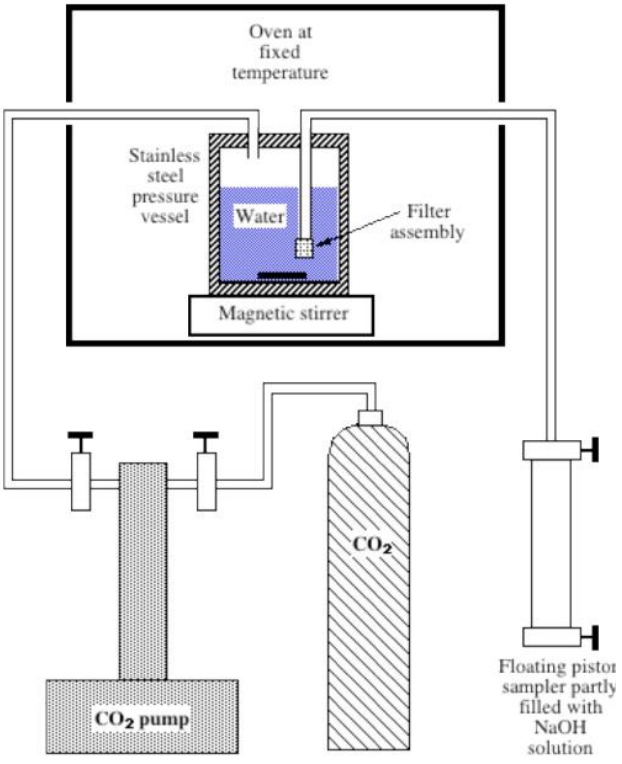

Figure 4: Rochelle et al. (2002) experimental setup [22]

The dissolved CO_2 was then stabilised by reacting it with 4M NaOH solution under experimental pressure and room temperature.

$$CO_{2(aq)} + NaOH = Na^+ + H^+ + CO_3^{2-} \quad (5)$$

All the carbonic species were converted to CO_3^{2-} due to the high pH of the solution and the CO_3^{2-} remained stable so long as the NaOH present was in excess. The solution could then be depressurised without any degassing and the CO_3^{2-} could be analysed, (using titration on a Radiometer VIT90 Video Tirtrator with ABU93 Triburette and SAM90 Sample Station) to provide a measurement of total dissolved CO_2. The addition of the NaOH solution caused dilution of the CO_2 solution and so a correction factor was needed in the form of a dilution factor which was either based on measured Na^+ content (for distilled water) or Cl^- content (for Utsira porewater).

The experimental conditions varied from 291-353K and 80-120 bar with the majority of the data being generated under the reservoir conditions in the Utsira formation at Sleipner (310K and 100 bar). Using distilled water, the measured CO_2 solubility values were roughly 10% lower than expected. However, they did follow the general trend of previous studies. [23,24,25] The reasoning behind the drop in CO_2 solubility was not clear. However, the authors did not take into account compressibility and expansivity corrections as they believed that cooling the solution would have an insignificant effect on volume of the solution, and this may have caused the lower than expected results. At 210K and 100 bar, the CO_2 solubility was 5.1g of CO_2 per 100g distilled water. [22] When measuring CO_2 solubility in the synthetic Utsira porewater, the results were comparable to that of previous work and lower than the results for distilled water. [26] Under the same conditions as for the distilled water, the CO_2 solubility was 4.5g per 100g Utsira porewater. [22]

3.2 Solubility of CO_2 in Aqueous Solutions of NaCl

The following year, Bando et al. (2003), studied the solubility of CO_2 in aqueous solutions of NaCl at (30 to 60) °C and (10 to 20) MPa. [27] The apparatus used (Figure 6) was made up of a high-pressure vessel (with a max pressure of 700 bar), two pressure transducers with different pressure ranges, an agitator, a pump for pressurising the water, an amplifier, a 50cm^3 sample cylinder and a CO_2 gas cylinder. Additionally, there was a gravimetric balance used to measure the mass of the samples collected. Experiments were run at temperature of 30°C, 40°C, 50°C and 60°C, pressure of 100 bar, 250 bar and 200 bar and 0, 0.0099, 0.02 and 0.03 NaCl mass fractions.

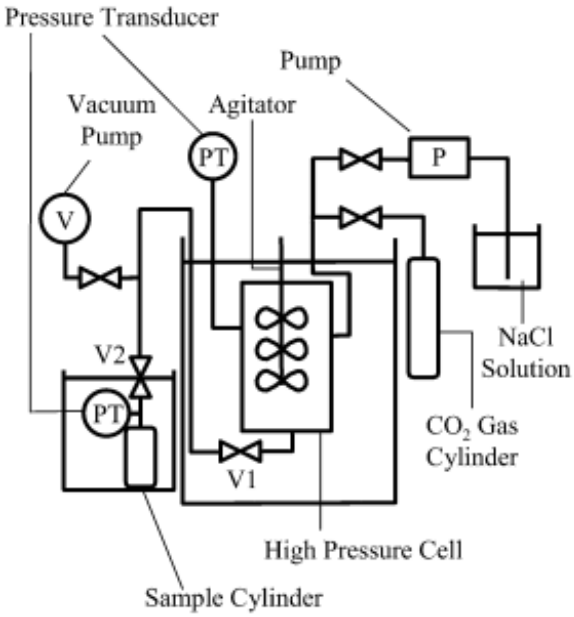

Figure 5: Bando et al. (2003) experimental setup [27]

Once the high-pressure vessel had been evacuated, CO_2 was injected to a pressure of approximately 10 bar. At this point, the aqueous NaCl solution was pumped into the vessel for 1 hour, while undergoing mixing by an agitator, and then left in the vessel while the temperature and pressure stabilised, which took about 2 hours. This was repeated until experimental conditions were achieved. Once the experimental conditions had been achieved,

the dissolved CO_2 solution was flashed into the sample cylinder. This was done until the pressure within the sample cylinder reached 10 bar. No degassing occurred due to the pressure of the vessel remaining constant throughout the extraction procedure. Once the sample had been collected, the sample cylinder was disconnected and cooled in an ice bath until it reached 0°C. The mass and pressure of the cylinder was then measured and used to calculate the CO_2 solubility in the aqueous NaCl solution. Some of the results obtained by Bando et al. (2003) can be seen in Figures 2 and 3. [12] According to the authors, the CO_2 solubility results obtained were in good agreement (within 0-6.4%) with previous work. [28,29,30,31]

3.3 Solubilities for Binary Systems of CO_2 + Water and CO_2 + Brine

Unlike with Bando et al. (2003), Li et al. (2004) developed a system for measuring the solubility of CO_2 in brine. [17] Their method used apparatus (Figure 7) similar to that of a PVT system with a 500cm^3 PVT cylinder, a high-pressure Ruska pump, a high-pressure CO_2 cylinder, a densitometer, a gasometer and a back pressure regulator (BPR), as shown in Figure 7. The PVT cylinder was situated in an air bath which could be rocked to accelerate the equilibrium process.

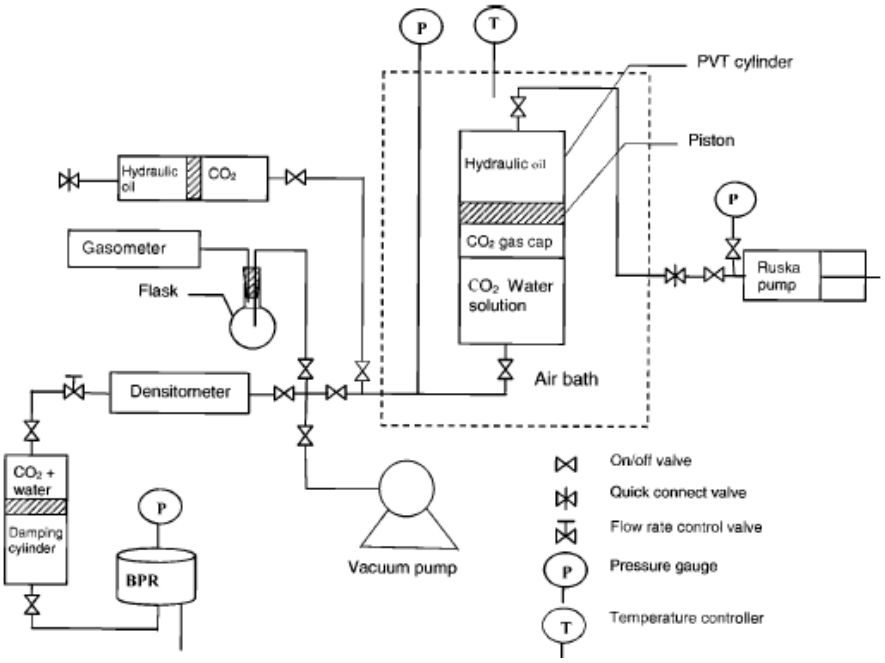

Figure 6: Li et al. (2004) experimental setup [17]

CO_2 was injected into the PVT cylinder, which contained a 450cm^3 sample of water. The amount of CO_2 needing to be injected was estimated by using data from Chang et al (1998). [32] An additional 30% CO_2 was injected into the PVT cylinder to ensure that there would be a gas cap at equilibrium. Once the CO_2 had been injected, the cylinder was pressurised and rocked, accelerating the equilibrium process. Equilibrium was assumed to have been reached when the pressure within the cylinder had remained constant for over 5 hours. Once equilibrium was reached, a 20cm^3 solution sample was extracted and collected in a flask. The mass of the sample was then measured and the gasometer was used to measure the CO_2 that evolved due to degassing, under ambient conditions. Using the mass of the solution and the volume of evolved CO_2, the CO_2 solubility could be calculated with the following equation:

$$R = \frac{n_g}{(m_g + m_w)/\rho_s} \quad (5)$$

Where R corresponds to the solubility of CO_2(aq), m_w is the mass of water, m_g is the mass of CO_2, n_g is the number of moles of CO_2 and ρ_s is the density of CO_2(aq) in solution under

saturation pressure. As with Bando et al. (2003), the results of Li et al (2003) are shown in Figures 2 and 3. [12] The authors do state that this method of calculation is only suitable for aqueous solutions that are near neutral. In addition, Yan et al (2011) have not used these data when creating a comprehensive review of previous experimental data, as they stated that the authors did not take into account dissolved CO_2 contained within the aqueous solution at atmospheric pressure. [33]

3.4 CO_2 solubility in NaCl Brine

The work by Yan et al. (2011), which included a comprehensive review of previous experimental data, measured CO_2 solubility and brine density using a modified high pressure PVT apparatus. [33] This apparatus (Figure 8) consisted of a DBR-JEFRI windowed equilibrium cell, an air bath, an Anton Paar high pressure density meter DMA 512, high pressure pycnometers (for sampling) and an ISCO displacement pump. The equilibrium cell was mounted upon a rocking device which accelerated the equilibrium process and also allowed for the cell to be put in the top-down and upright positions so that both heavy and light phases could be sampled. For phase sampling, the phase in question was discharged under constant pressure from the outlet located at the top of the cell.

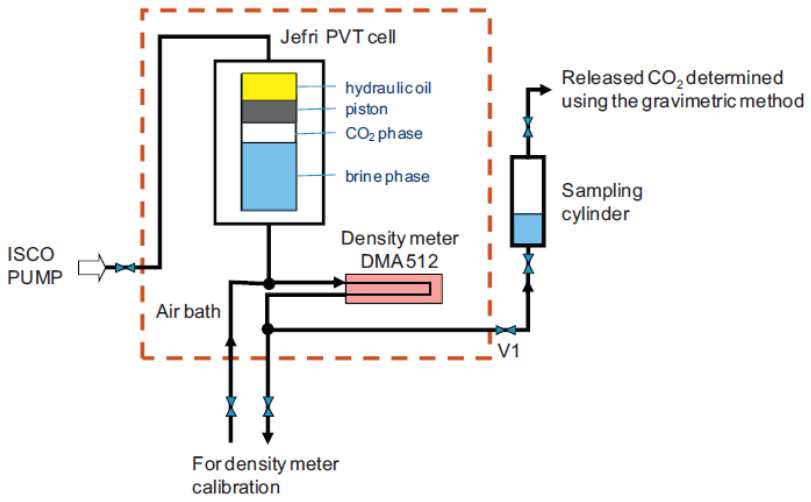

Figure 7: Yan et al. (2011) experimental setup [33]

The CO_2 and brine were sequentially injected into the equilibrium cell and the pressure and temperature were increased to the experimental values. The CO_2-brine mixture was then rocked for 2 hours and left overnight to reach equilibrium. Once the mixture had reached equilibrium, a brine-phase sample was extracted, through a density meter, into a pre-weighed sampling cylinder. The single phase brine was then flashed into two phases within the sampling cylinder and cooled. The weight of the cylinder was then measured and the amount of CO_2 dissolved in the sample was determined by slowly releasing the dissolved gas from the top of the cylinder. This was done until no more gas could be released, at which point the sampling cylinder was weighed again. The total volume of dissolved CO_2 within the brine sample was calculated by adding together the amount of CO_2 in the gas phase within the cylinder, the volume of CO_2 released from the cylinder and the dissolved CO_2 remaining in the sampling cylinder under atmospheric conditions.

According to the authors, the experimental method used in this work provided CO_2 solubility measurements that were in good agreement with literature data, as can be seen in Figure 9, and hence, showed the merits of using this method for measuring CO_2 solubility in brine at high pressures. CO_2 solubility and the associated CO_2-saturated brine densities were measured from 50-400 bar, at 323K, 373K and 413K and 0, 1 and 5M NaCl.

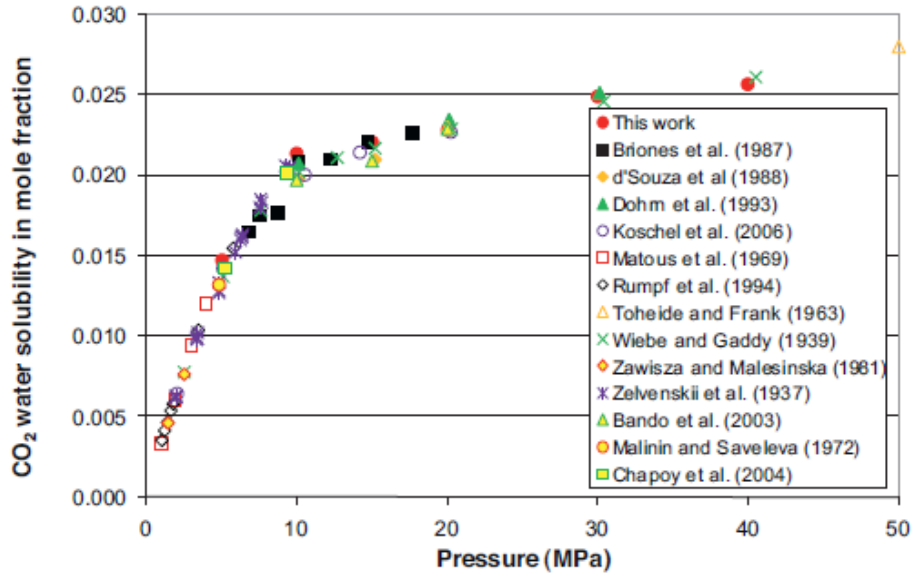

Figure 8: CO_2 solubility in water at 323K. Comparison of Yan et al. (2011) data with that of the literature [33]

3.5 Water Solubility of CO_2 under Supercritical and Subcritical Conditions

In 2003, Sabirzyanov et al. (2003) published their experimental setup (Figure 5), which comprised of a gas cylinder containing the gas that would be examined, 4 high pressure valves, a deadweight gauge, a Bourdon pressure gauge, a high-pressure mercury seal, a vacuum pump, a ball, a tee and a heat-insulated high-pressure autoclave. [34] The experimental pressure was obtained using both a hydraulic press and a hydraulic amplifier which was part of the deadweight gauge. The heat-insulated high-pressure autoclave was heated to the desired temperature using 3 Nichrome heaters. The autoclave used was a stainless steel cylinder with a sealed top cover that included a built-in high-pressure valve that could be used to isolate the vessel during agitation and equilibration. The autoclave also had a valve built in to the bottom of the vessel which was used to sample the liquid phase.

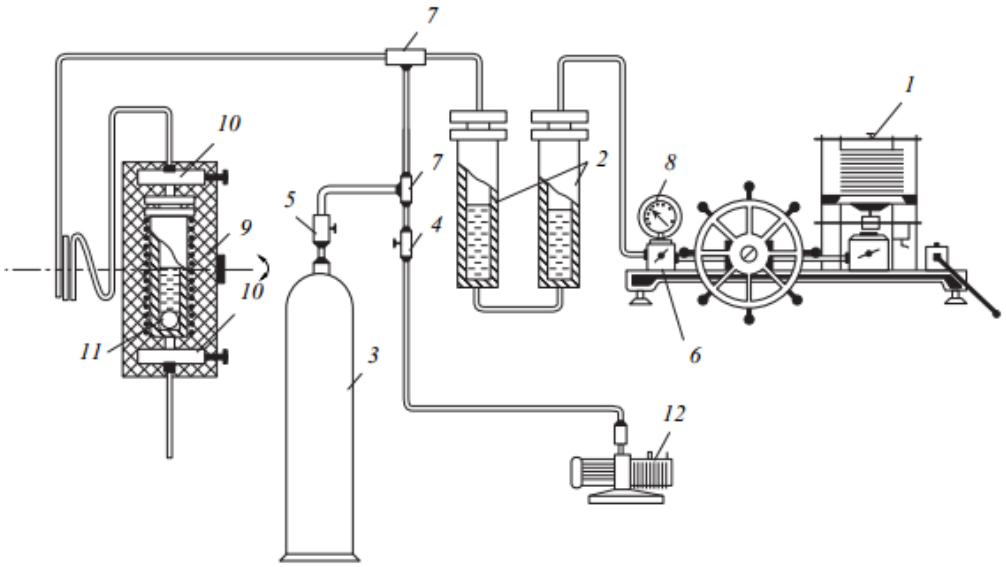

Figure 9: Sabirzyanov et al. (2003) experimental setup. (1) MP-2500 deadweight gage, (2) mercury seal, (3) gas cylinder, (4–6, 10) high-pressure valves, (7) tee, (8) standard pressure gage, (9) heat-insulated high-pressure autoclave, (11) ball, and (12) vacuum pump [34]

During the experiment, perfect mixing of the phases was obtained by rocking the autoclave about its horizontal axis, twice per minute, through an angle of 160°C. The mixing was further promoted by the inclusion of a perforated ball which had been placed in the vessel. The equilibrium point was determined from pressure variations measured from within the vessel. Once equilibrium was reached, the vessel was held in an upright position for 1-1.5 hours. During sampling, gas was injected into the vessel from the head space of the mercury seal, to maintain constant pressure. The samples were collected in a number of weighed ampoules and the gas, which was released as the sample was throttled through the high-pressure valve, was collected and its volume measured. Taking the measured volume of gas and weight of the liquid sample, the solubility of the CO_2 in water was determined. As with Bando et al. (2003) and Li et al. (2004), the results obtained by Sabirzyanov et al. (2003) can be seen in Figures 2 and 3. [12] The overall recorded error was reported to be 3%. [34] The authors reported that they had difficulty sampling the liquid phase from the bottom of the vessel under certain conditions due to the CO_2 being denser than water. Their results are also

reported to be within 7% of that of previous work, which is relatively high and brings into question the accuracy of this method. [35]

3.6 CO_2 and CH_4 Solubilities in Ternary Systems with Water.

Qin et al. (2008) developed an experimental method to calculate CO_2 and CH_4 solubility in a ternary system with water. [36] However, this method could also be used to simply measure CO_2 solubility in water and brine. The solubility experiments took place within a custom designed reaction cell which featured a 200cm^3 capacity titanium-lined autoclave. Contained within the titanium closure there were three compression fittings which accommodated a thermocouple and two titanium sampling tubes. There was also an additional thermocouple attached to the autoclave base. The reaction cell was fitted to a 180° rotating furnace, where sampling could be performed in either an inverted or upright position.

CO_2 and water were mixed within the cell at a rotation rate of 6 times per minute. Depending on the pressure and temperature, the mixture was allowed to equilibrate over a period of 8-36 hours. Once equilibrium had been reached, the rotator was turned off and left in the inverted position for roughly 30-60 minutes to allow complete separation of the liquid and vapour phases. The CO_2-water phase was extracted through a gastight syringe which contained approximately 1-2 cm^3 of 17% NaOH solution to stabilise the dissolved CO_2 and convert the carbonic species to CO_3^{2-} and HCO^{3-} and hence eliminate CO_2(aq). To prevent degassing, the experimental pressure and temperature was kept near constant during sampling. The amount of dissolved CO_2 contained within the water, and hence the CO_2 solubility, was measured through coulometric titration. This was done using a UIC Coulometric model CM5012 which was standardised by $CaCO_3$ solutions. The CO_2 solubility data obtained were validated by comparison with the Duan and Sun (2003) model. [14] The measured CO_2 solubility data at 375K were slightly lower than that contained within the Duan and Sun (2003) model,

deviating by less than 4%. This was still considered, by the authors, to be in good agreement with previous results and validated their experimental method. [36]

3.7 CO_2 Solubility in Aqueous Solutions of $CaCl_2$ and $MgCl_2$

The most recent work on measuring CO_2 solubility under reservoir conditions was performed by Tong et al. (2013). [37] Their method was based upon visual observation, alongside quantitative measurements of pressure, temperature and composition. This avoided the complications associated with phase sampling and analysis, and allowed for the rapid collection of reliable data.

The experimental setup for this work is shown in Figure 9. CO_2 was injected into a windowed cell and allowed to reach equilibrium, at which point both the pressure and temperature were measured, so that, an equation of state (in conjunction with the known volume) could be used to calculate the mass of CO_2 present. Upon calculating the mass of CO_2 present, the brine was injected using a syringe pump, and stirred until complete dissolution was achieved. The mass of the injected brine was determined through knowledge of the initial and final volume, pressure and temperature in the pump cylinder, along with the brine density under said conditions.

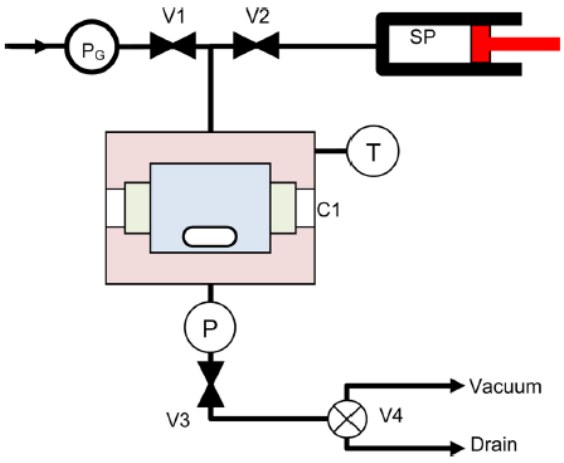

Figure 10: Tong et al. (2013) experimental setup [37]

The bubble point can be determined through visual observation at high pressures. Once the brine had been injected and full stabilisation had occurred within the cell, the pressure was gradually decreased until bubbles appeared. This was done by removing fresh brine, not in contact with the CO_2, from the inlet line. The phase boundary under high pressure conditions is first observed as slight temporal and spatial variations in the light passing through the solution and not through bubble formation. The reasoning behind this is that under these conditions the brine and the CO_2-rich phase densities are comparable.

Once the bubble point has been observed, the composition of the solution, which is expressed as the salt-free mole fraction of dissolved gas, can be determined through knowledge of the masses of both the brine and CO_2 present. In addition, the bubble point density of the CO_2-saturated brine can also be calculated since the cell volume is known. The results obtained through this method are in good agreement with previous work (within ±2-5%) and with the Duan et al (2006) model which can be seen in Section 5. [15,30,38] This method was used to measure CO_2 solubility in aqueous solutions of $CaCl_2$ and $MgCl_2$ and successfully expanded the knowledge on how CO_2 solubility is affected by pressure, temperature and salinity in these aqueous solutions. It was found that there is a stronger salting out effect in systems containing divalent cations than those containing monovalent cations (NaCl/KCl). In addition, the solubility of CO_2 in $MgCl_2$ and $CaCl_2$ solutions of the same molality were comparable. It was therefore concluded that ion charge is considerably more important, in regards to the salting out effect, than ion size.

3.8 Summary

This section has reviewed a variety of different methods of measuring CO_2 solubility under reservoir conditions and how the experimental setup used has evolved over the years. Although all these methods have all generally agreed with the literature and follow the same

trends there are clearly large deviations in results, with some methods appearing far more effective than others. Due to being in good agreement with results from previous work, as well as the Duan and Sun CO_2 solubility model, the work by Tong et al. (2013) seems to be the most accurate at measuring CO_2 solubility in brine under reservoir conditions. This will be emphasised in the following sections which review geochemical modelling of CO_2 solubility in brine and how the results obtained through modelling compare with those of the experimental work.

4 Geochemical Modelling

There are a variety of geochemical modelling software packages that can be used to calculate CO_2 solubility in brine under reservoir conditions. However for the purposes of this paper, only the three that were used to perform the geochemical modelling provided in Section 5, will be analysed, namely: (i) a general geochemical software program known as PHREEQC; (ii) HydraFLASH, an in-house software developed at Heriot-Watt University, that allows the user to change the Equation of State (EoS) used; and (iii) the previously mentioned Duan and Sun CO_2 solubility model, which is the most widely used model for calculating CO_2 solubility in brine.

4.1 PHREEQC

PHREEQC is a general geochemical software program that requires very little prior modelling experience but can be applied to most hydrochemical environments. [39] It is capable of saturation-index and speciation calculations as well as one-dimensional transport and batch-reaction calculations which involve reversible reactions, such as mineral gas, aqueous, surface-complexation, solid-solution and ion-exchange equilibrium. Batch-reaction calculations involving irreversible reactions are also possible, including kinetically controlled reactions, temperature changes, specified mole transfer of reactants and mixing of solutions.

In addition the software program is also capable of inverse modelling, which is used to find sets of gas and mineral mole transfers that affect water composition. [40] Previous work by Liu (2012) concluded that PHREEQC cannot be used to accurately predict experimental results. [41] This is because complex ion exchange models are not considered, it does not take into account uncertainties in thermodynamic constants and it makes simplified assumptions related to steady-state flow [42]. It can, however, be used to demonstrate general trends.

4.2 HydraFLASH

HydraFLASH is an in-house software developed by the HYDRAFACT group at Heriot-Watt University. It is a PVT and thermodynamic prediction software which, allows modelling of multicomponent, multiphase aqueous and hydrocarbon systems in the presence and absence of hydrates and inhibitors. [43] Although mainly used for modelling hydrocarbons for the oil and gas industry, it can be also used to calculate CO_2 solubility in brine. It is an effective tool for modelling CO_2 solubility as, unlike most geochemical models, HydraFLASH allows the user to change the EoS used for the calculations. This is important, as some EoS are more suited than others when calculating CO_2 solubility in brine. The EoS available are Soave-Relich-Kwong (SRK), Peng-Robinson (PR), Valderrama–Patel–Teja (VPT), Perturbed Chain form of the Statistical Associating Fluid Theory (PC-SAFT) and Simplified Cubic Plus Association (sCPA). [43]

The SRK EoS was developed in 1972 and was a modification of the Van der Waals (VdW) EoS. [44] The SRK EoS is very effective for predictions involving polar systems and is expressed as:

$$\left(P + \frac{\alpha a}{\tilde{v}(\tilde{v}+b)}\right)(\tilde{v} - b) = RT \quad (6)$$

At present, the PR EoS is the most popular EoS in the petroleum industry for use with natural gas systems. [45] The PR EoS is very similar to that of the SRK EoS but works slightly better at the critical point. This makes the PR EoS more effective with regards to gas/condensate systems, whereas the SRK EoS is superior for polar systems. Since the petroleum industry is more interested in gas/condensate systems than polar systems, the PR EoS is considered a superior EoS. [45] In addition, the PR EoS is used by PHREEQC. [40] The PR EoS is described as:

$$\left(P + \frac{\alpha a}{\tilde{v}^2 + 2b\tilde{v} - b^2}\right)(\tilde{v} - b) = RT \tag{7}$$

The VPT Equation of State (EoS) is a general phase equilibrium model which is based upon fugacity equality for each component in all phases. [46] The VPT EoS, used alongside non-density dependant (NDD) mixing rules, is used for modelling fluid phases. The combination of the VPT EoS and the NDD mixing rules results in an effective tool for modelling systems containing polar and non-polar compounds i.e. water and CO_2 systems. The VPT EOS is described as:

$$P = \frac{RT}{v - b} - \frac{a}{v(v+b) + c(v-b)} \tag{8}$$

The PC-SAFT EoS is expressed as the sum of the residual Helmholtz free energy terms that are a by-product of the different kinds of molecular interactions that occur within the system. [47] The residual Helmholtz free energy is described as the difference between the Helmholtz free energy and the Helmholtz free energy of the ideal gas (at the equivalent density and temperature). The PC-SAFT EoS can be accurately used to model complex CO_2 mixtures, for example those containing ionic liquids and amines.

The sCPA is a non-cubic EoS which, is based on the perturbation theory. [48] The sCPA EoS consists of two terms, the first is the SRK EoS (used to describe physical interactions) and the

second is a chemical expression by Wertheim (used to model hydrogen bonding compounds). The sCPA EoS is most effective when used on non-polar and only slightly polar systems. It also works well for a few hydrogen bonding systems. Its main applications are to study the compatibility of polymeric blends and the liquid to liquid equilibria resulting from water-soluble polymer solutions that contain hydrogen bonds which play crucial roles in the calculation of phase equilibira, as well as other related properties.

4.3 Duan and Sun CO_2 Solubility Model

The Duan and Sun CO_2 solubility model is a thermodynamic model which was first developed to calculate CO_2 solubility in both pure water and NaCl(aq) solutions in the temperature range of 273K to 533K, pressure range from 0 to 2000bar and an ionic strength ranging from 0 to 4.3m. [14] This model was then improved so that it could be used to calculate CO_2 solubility in aqueous solutions which contained, N^+, K^+, Mg^{2+}, Ca^{2+}, SO^{2-}_4 and Cl^-. [15] It also improved the models ability to calculate CO_2 solubility in pure water as well as in NaCl(aq) solutions.

The Duan and Sun model is unique in that it does not use any of the aforementioned EoS, for an EoS was developed specifically for the model. [14,15] Having its own EoS, specifically designed to calculate CO_2 solubility is the reason why the model is so widely used and why the vast majority of experimental results are compared with those produced from this model. The Duan and Sun model is more accurate when looking at CO_2 and pure water systems, as well as CO_2-water-salt systems, which is shown in the next section. However, for the CO_2-brine systems, the model looks at the overall salinity of the brine rather than the actual brine composition. Therefore, if it is necessary for the brine composition to be altered then geochemical software such as PHREEQC and HydraFLASH need to be used. How the geochemical models compare under different conditions is described in the following section.

5 Comparison between Modelling and Experimental Results

This section discusses the impact of choosing the correct EoS and compares the experimental methods for measuring CO_2 solubility by comparing the results with those calculated through geochemical modelling.

5.1 Choosing an Appropriate EoS

As described in the previously section, there are a multitude of EoS that HydraFLASH uses to calculate CO_2 solubility. The aforementioned PR EoS is the most popular EoS in the petroleum industry, due to its ability to accurately model gas/condensate systems. [45] It is also the EoS used by PHREEQC. [40] However, CO_2 solubility in brine is not described as a gas/condensate system, but it is rather a system containing polar and non-polar compounds. [49] Accordingly, the most appropriate EoS for systems containing polar and non-polar compounds is the VPT EoS. [46] Therefore, the VPT EoS should be the most suitable EoS for measuring CO_2 solubility in brine, which will be confirmed in this section.

Figures 11 and 12 show the results obtained when using different EoS and how they compare with the corresponding experimental work. They were produced by inputting the pressure, temperature and salinity data from Yan et al. (2011) and Li et al. (2004) into HydraFLASH and running the software. This was done five times, for each data set, keeping all the conditions constant and only altering the EoS used.

Figure 11 includes the results from Yan et al. (2011), where CO_2 solubility was measured in a CO_2-H_2O-NCl (1M) system at 323.2K under varying pressures. [33] Also present in the Figure are the results from the five different EoS that HydraFLASH can use. It can be seen that at low pressures it is difficult to distinguish between the different EoS. However, as the pressure

increases, the VPT results separate themselves from the rest and are comparable to the experimental results provided by Yan et al. (2011). [33]

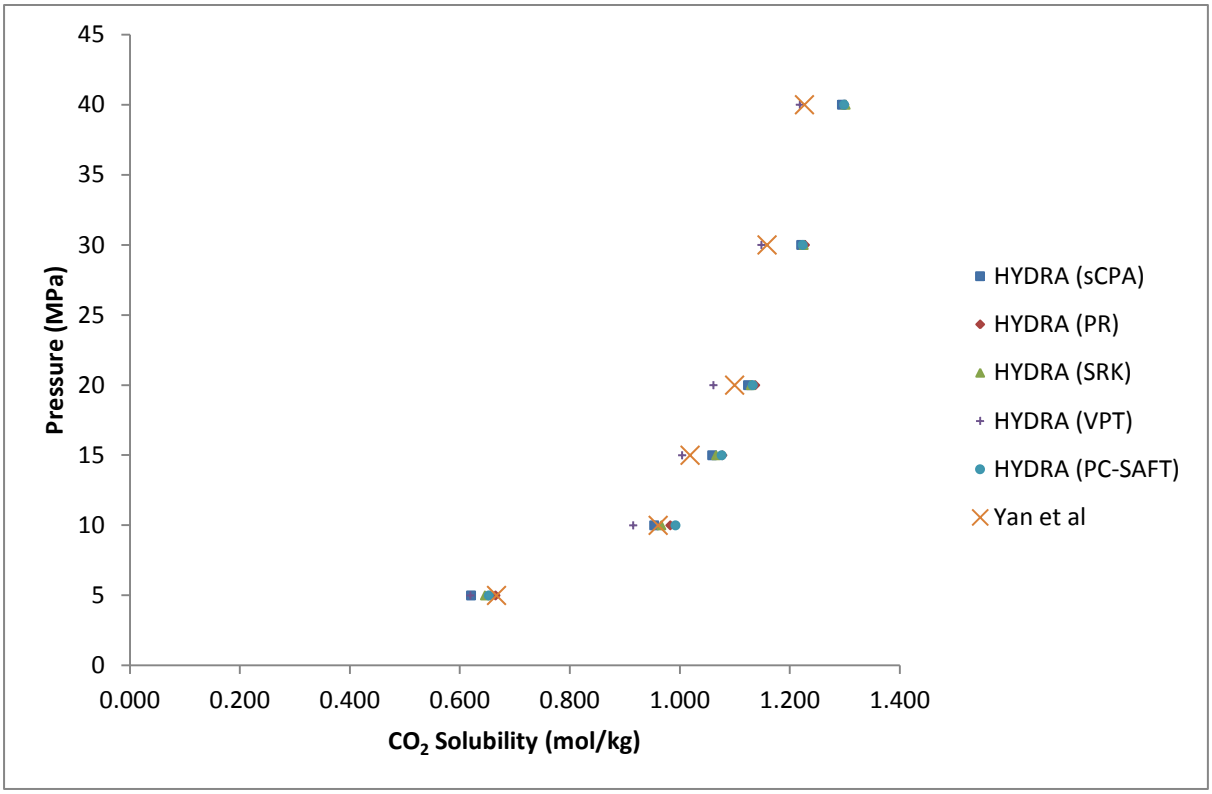

Figure 11: CO_2 solubility for CO_2-H_2O-NCl (1M) system at 323.2K using different EoS

The same trend can be seen in Figure 12, which compares the modelling results with those obtained by Li et al. (2004). [17] This system included CO_2 and brine from the Weyburn reservoir in Canada. In this case the pressure was varied under a constant temperature of 332.15K. As with Figure 11, the results are difficult to distinguish between at low pressures, but as the pressure increases it is clear that the VPT results are in agreement with those from the experimental work. The results from these two figures confirm that when considering systems containing polar and non-polar compounds, such as CO_2 and brine, the VPT is the superior EoS.

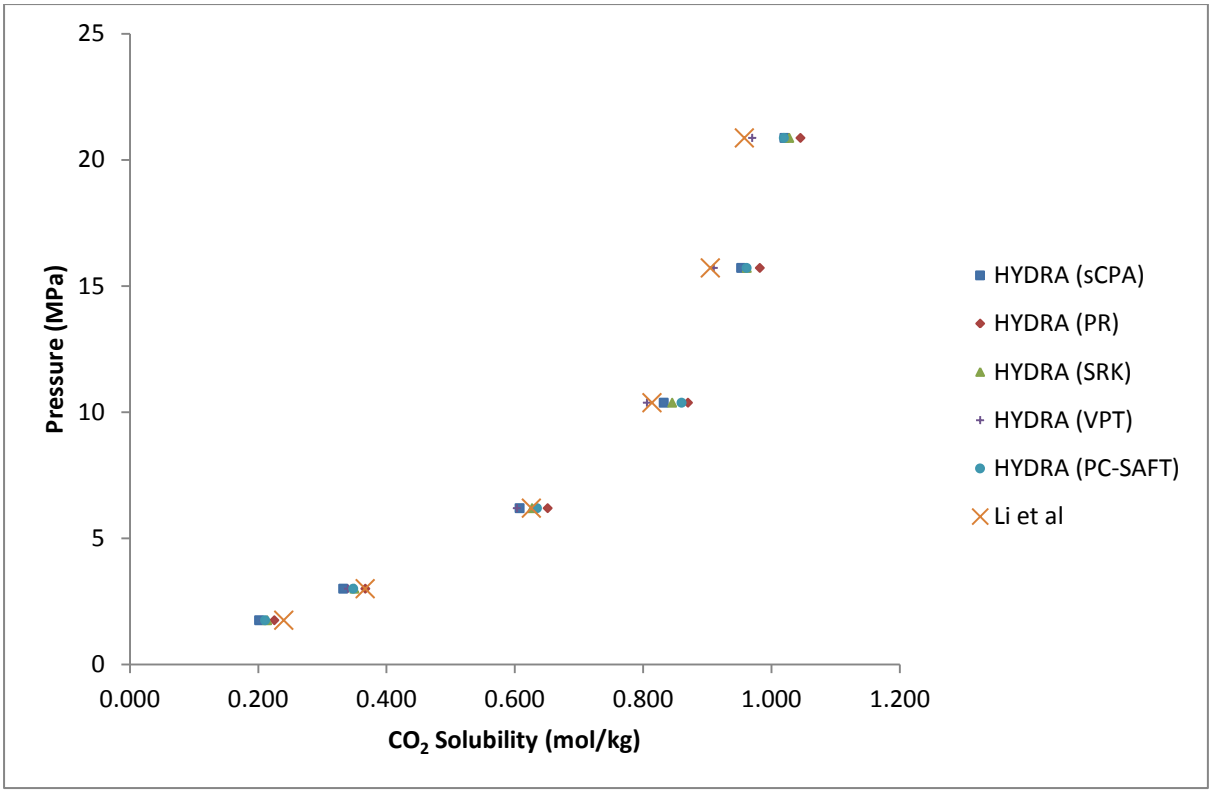

Figure 12: CO_2 Solubility for CO_2-Weyburn brine at 332.15K using different EoS

5.2 Comparison of the Geochemical Models

Section 4 discussed three different geochemical models that can be used to measure CO_2 solubility in brine, namely PHREEQC, HydraFLASH and the Duan and Sun CO_2 solubility model. Figures 13 and 14 provide a comparison of the different geochemical models. The figures were developed by using the same pressure, temperature and salinity data used to generate Figures 11 and 12. These data were input into PHREEQC, HydraFLASH (selecting only the VPT EoS this time) and the online CO_2 solubility calculator from Duan and Sun and compared once again with the results from Yan et al. (2011) and Li et al. (2004).

Figure 13 shows the experimental results of Yan et al. (2011) alongside the results from the Duan and Sun CO_2 solubility model, PHREEQC and HydraFLASH (using the VPT EoS). [33] In Section 4 it was stated that since the Duan and Sun model uses an EoS specifically designed to measure CO_2 solubility, in CO_2-water and CO_2-water-salt systems, it should

produce more accurate results when looking at these systems. This can be seen in Figure 13, as with increasing pressure, the CO_2 solubility results are in agreement with those of the experimental work. It is, however, very difficult to distinguish between the results from the Duan and Sun model and those from the HydraFLASH model, when using the VPT EoS. This shows the merits of using the HydraFLASH model when the correct EoS is selected. The results from PHREEQC on the other hand, do follow the correct trend. However, the accuracy of the results is far lower than that of the other two models. This is due to the fact that not only does it use the PR EoS, which, as previously stated, is designed for gas/condensate systems, it also ignores complex ion exchange models, does not take into account uncertainties in thermodynamic constants and makes simplified assumptions related to steady-state flow. [42] That being said, PHREEQC can still be used to show trends and is useful for those who require easy to use geochemical modelling software.

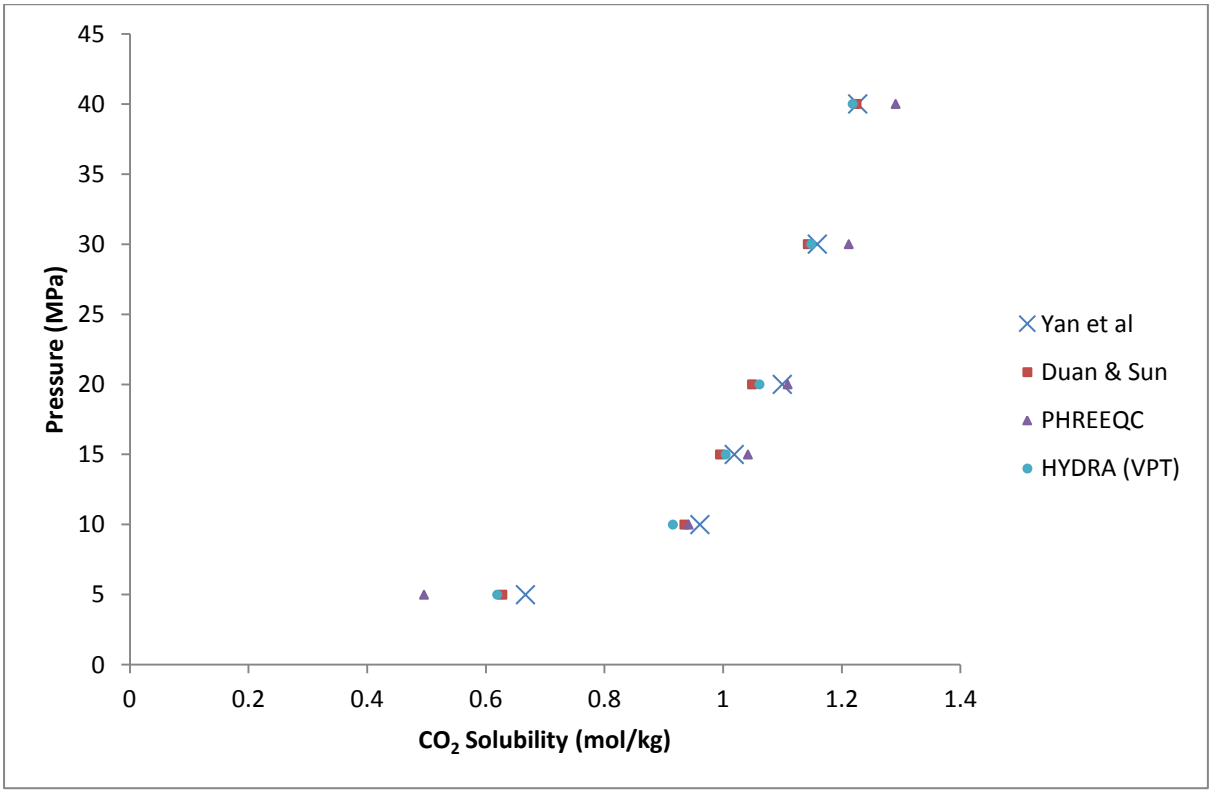

Figure 13: CO_2 solubility for CO_2-H_2O-NCl (1M) system at 323.2K using different geochemical models

The Duan and Sun model cannot be used for the Li et al. (2004) system, as it only allows for the total salinity of the brine to be inputted instead of the actual brine composition i.e. concentration of Ca^{2+}, Mg^{2+}, K^{+} ions. Therefore, Figure 14 only compares the experimental results to those obtained using PHREEQC and HydraFLASH. In this case the gap between the PHREEQC results and those of both HydraFLASH and the experimental work is relatively small at higher pressures. It is therefore possible that PHREEQC works better when looking at CO_2-brine systems.

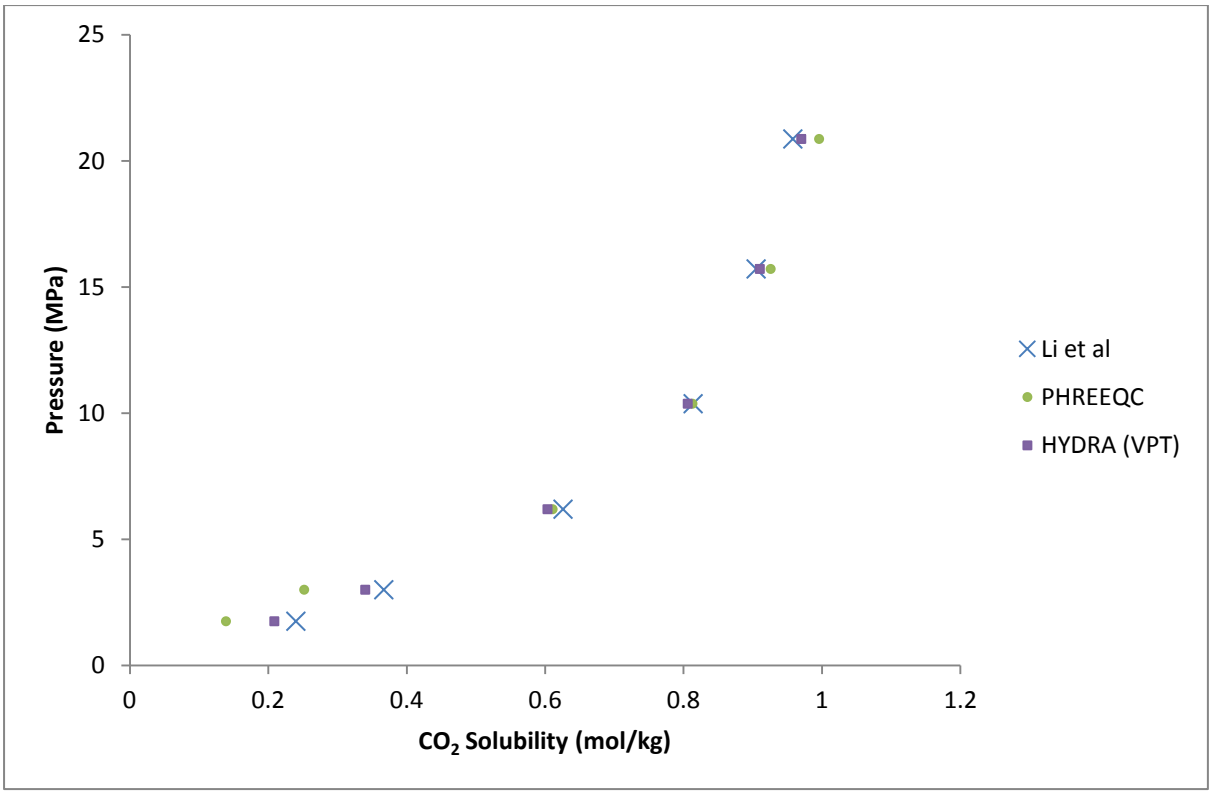

Figure 14: CO_2 solubility for CO_2-Weyburn brine at 332.15K using different geochemical models

In this section the work by Li et al. (2004) and Yan et al. (2011) has been compared to the results obtained through geochemical modelling. Both sets of results appear to be in good agreement with those of the modelling work. However, in both methods the experimental results do not correspond with those of the geochemical modelling at low pressures (as can be seen in Figures 13-14). Careful analysis of Figures 13-14 appears to show that the

experimental results of Yan et al. (2011) are in better agreement with the modelling results than those of Li et al. (2004). The reason for this was provided in Section 3 where it was stated that Yan et al (2011) did not use the data produced by Li et al. (2004) when creating their review of previous experimental data, due to the authors neglecting to take into account dissolved CO_2 contained within the aqueous solution at atmospheric pressure. [33] Therefore, it can be concluded that the experimental method developed by Yan et al. (2011) is more accurate at measuring CO_2 solubility than the one developed by Li et al. (2004).

5.3 Experimental Method Performance

In the summary of Section 3, it was stated that the work by Tong et al. (2013) seemed to be the most accurate at measuring CO_2 solubility in brine under reservoir conditions. Being the most recent attempt to develop a method of measuring CO_2 solubility under reservoir conditions, it is reasonable to assume that it would also be the most accurate, since the authors have been able to build upon previous methods. This section reviews the results obtained by Tong et al. (2013) and how they compare with both previous work and the results obtained through geochemical modelling.

Figure 15 shows CO_2 solubility in a CO_2-water system at 374K under varying pressures. The results included are those presented by Tong et al. (2013) and compared with the results obtained when the experimental conditions were input into the Duan and Sun online CO_2 solubility model as well as previous experimental work by Wiebe et al. (1939) and Prutton et al. (1945). [30,38,37] It should be noted that the work by Tong et al. (2013) and the Duan and Sun model are in very good agreement, but unlike with the work by Li et al. (2004) and Yan et al. (2011), the results by Tong et al. (2013) are also in good agreement with the Duan and Sun model at low pressures.

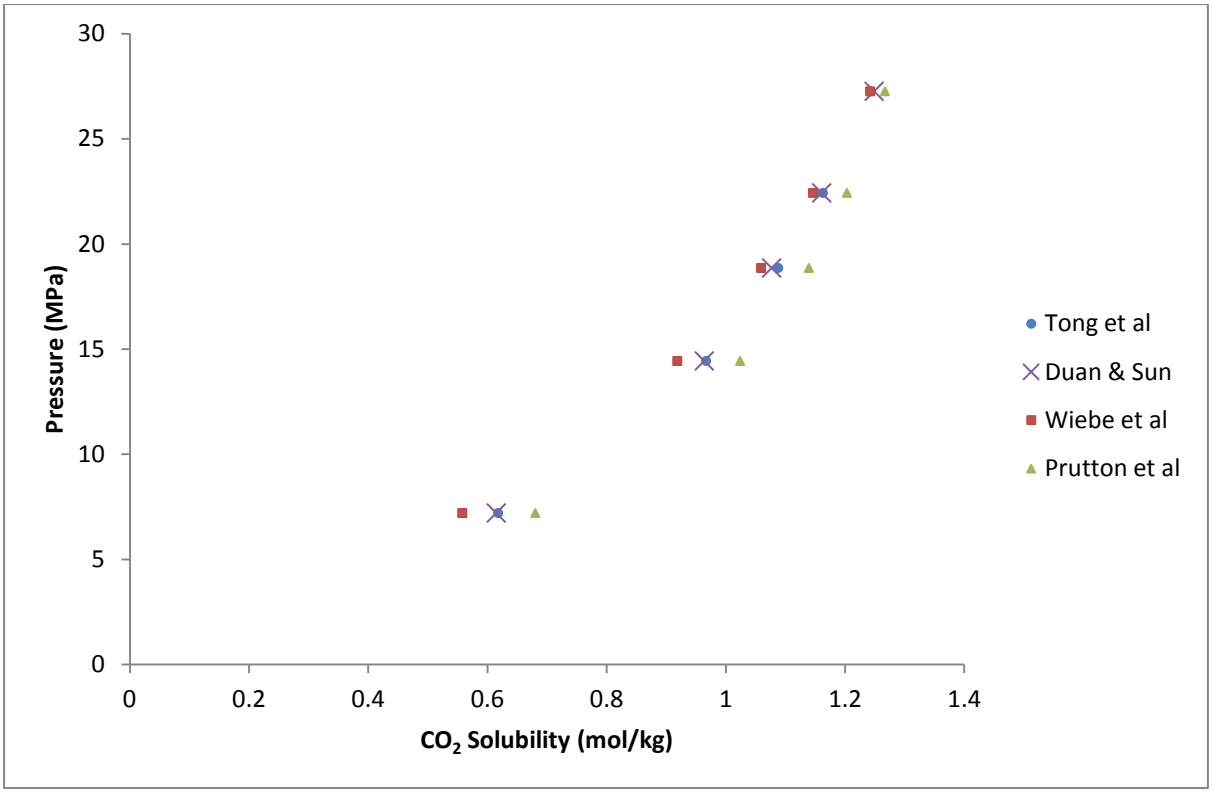

Figure 15: CO_2 solubility for CO_2+water system at 374K (experimental)

Figure 16 describes the same system (CO_2 + water system at 374K under varying pressures), but compares the results from Tong et al. (2013) with those of the three geochemical models discussed in this paper. Since this is just a CO_2-water system, although all the modelling results are in good agreement with those of the experimental work, the results from the Duan and Sun model show very little deviation from those of Tong et al. (2013).

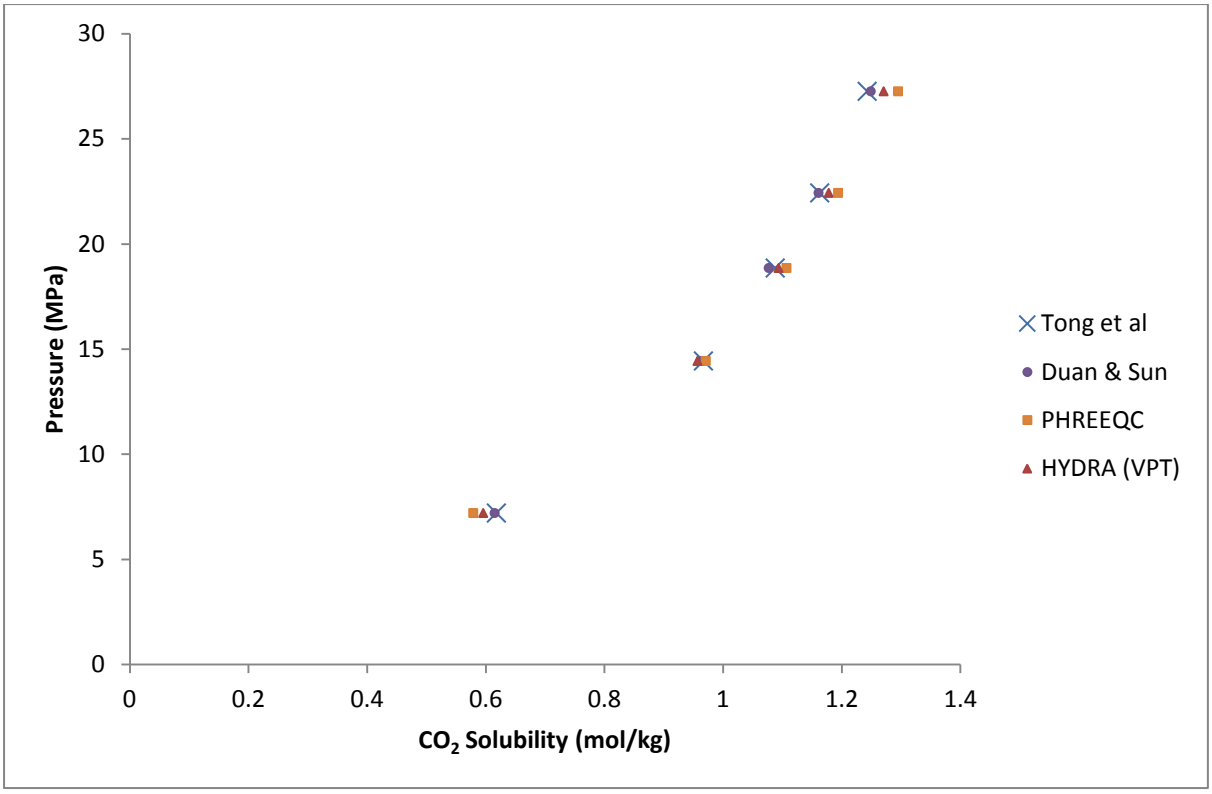

Figure 16: CO_2 solubility for CO_2+water system at 374K (modeling)

It is clear that the experimental procedure developed by Tong et al. (2013) is currently the most accurate at measuring CO_2 solubility under reservoir conditions. This is confirmed by the fact that not only are the results in very good agreement with those of the geochemical modelling, but unlike with some of the previous works, the results from Tong et al. (2013) are comparable with those obtained through modelling at low pressures as well. Furthermore, this method has been used to measure CO_2 solubility in aqueous solutions of $CaCl_2$ and $MgCl_2$ and has successfully expanded the knowledge on how CO_2 solubility is affected by pressure, temperature and salinity in these aqueous solutions. [37]

6 Conclusions

This paper has provided an in-depth review of the work carried out over recent years on measuring CO_2 solubility under reservoir conditions. Although all of the results obtained through these methods follow the correct trends, some are far more accurate than others.

There have, however, been large improvements as the years have progressed and the work by Yan et al. (2011) and Tong et al. (2013) are in very good agreement with results obtained through geochemical modelling. [33,37] Moreover, the procedure developed by Tong et al. (2013) produces results that are in good agreement with the literature at both high and low pressures and hence can be considered the more effective of the two.

In regards to geochemical modelling, three models were reviewed, namely PHREEQC, HydraFLASH and the Duan and Sun CO_2 solubility model. It was concluded that for systems including only CO_2 and water or CO_2, water and salt, the Duan and Sun model was the most accurate at calculating CO_2 solubility. This is mainly because it has an EoS designed specifically to perform CO_2 solubility calculations. [50] PHREEQC on the other hand is simple to use, but it cannot accurately predict experimental results and can only really be used to show trends. Finally, HydraFLASH was shown to be a very effective all round model, as it can match the accuracy of the Duan and Sun model in CO_2-water and CO_2-water-salt systems, and also has the ability to calculate CO_2 solubility in brine. The only requirement of HydraFLASH to produce accurate results that are in agreement with the experimental work, is that the correct EoS is chosen. This paper also reviewed the importance of selecting the right EoS and it was concluded that for a system containing polar and non-polar compounds, such as CO_2 in water, the Valderrama–Patel–Teja EoS is the most effective. [46]

Acknowledgements

To be inserted.

References

1. IEA. Key World Energy Statistics 2014. [Online].; 2014 [cited 2015 February 24. Available from: http://www.iea.org/publications/freepublications/publication/keyworld2014.pdf.

2. IEA. Key World Energy Statistics 2013. [Online].; 2013 [cited 2014 January 6. Available from: http://www.iea.org/publications/freepublications/publication/KeyWorld2013_FINAL_WEB.pdf.

3. Tyndall Centre for Climate Change Research. CO2 emissions set to reach new 40 billion tonne record high in 2014. [Online].; 2014 [cited 2015 February 24. Available from: http://www.tyndall.ac.uk/communication/news-archive/2014/co2-emissions-set-reach-new-40-billion-tonne-record-high-2014-0.

4. NETL. Carbon Dioxide Enhanced Oil Recovery: Untapped Domenstic Energy Supply and Long Term Carbon Storage Solution. Morgantown:; 2010.

5. USEPA. Climate Change Indicators in the United States. [Online].; 2012 [cited 2014 January 7. Available from: http://www.epa.gov/climatechange/science/indicators/index.html.

6. IPCC. Special report on carbon dioxide capture and storage. Cambridge:; 2005.

7. IEA. Overview. [Online]. [cited 2014 January 13. Available from: http://www.iea.org/textbase/npsum/ccsSUM.pdf.

8. Bachu S, Bonijoly D, Bradshaw J, Burruss R, Holloway S, Christensen NP, et al. CO2 storage capacity estimation: Methodology and gaps. International Journal of Greenhouse Gas Control 1. 2007;: p. 430-443.

9. Garcia SKAMVMM. Underground carbon dioxide storage in saline formations. Waste and Resource Management 163. 2010.

10. Druckenmiller ML, Maroto-Valer MM, Hall M. Investigation of carbon sequestration via induced calcite formation in natural gas well brine. Energy & Fuels 20. 2006;: p. 172-179.

11. Rosenbauer RJ, Koksalan T. Experimental determination of the solubility of CO2 in electrolytes: application to CO2 sequestration in deep, saline aquifers. The Geological Society of America 2. 2002;: p. 304.

12. Iqlauer S. Dissolution Trapping of Carbon Dioxide in Reservoir Formation Brine - A Carbon Storage Mechanism. In Nakajima H, editor. Mass Transfer - Advanced Aspects.: InTech; 2011. p. 233-262.

13. Averill BA, Eldredge P. Effects of Temperature and Pressure on Solubility. In Principles of General Chemistry.; 2012. p. 1577-1589.

14. Duan Z, Sun R. An improved model calculating CO2 solubility in pure water and aqueous NaCl

solutions from 273 to 533K and from 0 to 200 bar. Chemical Geology 193. 2003;: p. 257-271.

15. Duan Z, R S, Zhu C, Chou IM. An improved model for the calculation of CO2 solubilities in squeous solutions containing Na+, K+, Ca2+, Mg2+, Cl- and SO42-. Marine Chemistry 98. 2006;: p. 131-139.

16. Nighswander JA, Kalogerakis N, Mehrotra K. Solubilities of carbon dioxide in water and 1 wt% NaCl solution at pressure up to 10 MPa and temperatures from 80 to 200C. Journal of Chemical & Engineering Data 34. 1989;: p. 355-360.

17. Li Z, Dong M, Li S, Dai L. Densities and solubilities for binary systems of carbon dioxide + water and carbon dioxide + brine at 59C and pressure to 29 MPa. Journal of Chemical & Engineering Data 49. 2004;: p. 1026-1031.

18. Kiepe J, Horstmann S, Fischer K, J G. Experimental determination and predicition of gas solubility data for CO2 + H20 mixtures containing NaCl or Kcl at temperatures between 313 and 393K and pressures ip to 10 MPa. Industrial and Engineering Chemistry Research 41. 2002;: p. 4393-4398.

19. Rumpf B, Nicolaisen HOC, Maurer G. Solubility of carbon dioxide in aqueous solutions and sodium chloride: experimental results and correlation. Journal of Solution Chemistry 23. 1994;: p. 431-448.

20. Gross PM. The "Salting out" of Non-electrolytes from Aqueous Solutions. Chemical Reviews. 1933 August; 13(1).

21. Lara TFC. Design and Testing of an Apparatus to Measure Carbon Dioxide Solubility in Liquid Foods. Florida:; 2008.

22. Rochelle CA, Moore YA. The solubility of supercritical CO2 into pure water and synthetic Utsira porewater. Keyworth, Nottingham: British Geological Survey; 2002.

23. Kuk MS, Montagna J. Solubility of oxygenated hydrocarbons in supercritical carbon dioxide. Chemical Engineering at Supercitical Fluid Conditions. 1983.

24. Wiebe R. The binary system carbon dioxide-water under pressure. Chemical Engineeering at Supercritical Fluid Conditions. 1941 December; 29(3).

25. Wiebe R, Gaddy VL. Vapour phase composition of carbon dioxide-water mixtures at various temperatures and at pressures up to 700 atmospheres. Journal of the American Chemical Society. 1941 February; 63(2).

26. Czernichowski-Lauriol I, B S, Rochelle C, Bateman K, Pearce J, Blackwell P. The underground disposal of carbon dioxide. Keyworth, Nottingham: British Geological Survey; 1996.

27. Bando S, Takemura F, Nishio M, Hihara E, Akai M. Solbulity of CO2 in aqueous solutions of NaCl at (30 to 60)C and (10 to 20) MPa. Journal of Chemical & Engineering Data 48. 2003;: p. 576-579.

28. D'Souza R, Patrick JR, Teja AS. High-pressure phase-equilibria in the carbon-dioxide normal-hexadecane and carbon-dioxide water-systems. Canadian Journal of Chemical Engineering. 1988; 66.

29. Gillespie PC, Wilson GM. Vapor-Liquid and Liquid-Liquid Equilibria. Gas Processors Association Research Report. 1982; 1(73).

30. Wiebe R, Gaddy VL. The solubility of carbon dioxide in water at 50, 75 and 100C, at pressures to 700 atm. Journal of the American Chemical Society. 1939; 61.

31. Wiebe R, Gaddy VL. The solubility of carbon dioxide in water at various temperature from 12 to 40C and at pressures to 500 atm. Journal of the American Chemical Society. 1940; 62.

32. Change YB, Coats BK, Nolen JS. A Compositional Model for CO2 Floods Including CO2 Solubility in Water. SPE Reservoir Evaluation & Engineering. 1998 April; 1(2).

33. Yan W, Huang S, Stenby EH. Measurement and modeling of CO2 solubility in NaCl brine and CO2–saturated. International Journal of Greenhouse Gas Control. 2011 September; 5(6).

34. Sabirzyanov AN, Shagiakhmetov RA, Gabitov FR, Tarzimanov AA, Gumerov FM. Water solubility of carbon dioxide under supercritical and subcritical conditions. Theorectical Foundations of Chemical Engineering 37. 2003;: p. 51-53.

35. King MB, Mubarak A, Kim JD, Bott TR. The mutual solubilities of water with supercritical and lqiuid carbon dioxide. Journal of Supercritical Fluids. 1992 December ; 5(4).

36. Qin J, Rosenbauer RJ, Duan Z. Experimental Measurements of Vapor–Liquid Equilibria of the H2O + CO2 + CH4 Ternary System. Jounral of Chemical and Engineering Data. 2008 May; 53(6).

37. Tong D, Truslet MJP, Vega-Maza D. Solubility of CO2 in Aqueous Solutions of CaCl2 or MgCl2 and in a Synthetic Formation Brine at Temperatures up to 423 K and Pressure up to 40 MPa. Jounral of Chemical and Engineering Data. 2013 May; 58(7).

38. Prutton CF, Savage RL. The solubility of carbon dioxide in calcium chloride-water solutions at 75, 100, 120 C and high pressures. Journal of the American Chemical Society. 1945; 67.

39. Gundogan O, Mackay E, Todd A. Comparison of numerical codes for geochemical modelling of CO2 storage in target sandstone reservoirs. Chemical Engineering Research and Design 89. 2011;: p. 1805-1816.

40. Parkhurst DL, Appelo CAJ. User's guide to PHREEQC (version 2) - a computer program for speciation, batch-reaction, one-dimensional transport, and inverse geochemical calculations Denver: U.S. Geological Survey; 1999.

41. Liu Q. Investigation of mineral trapping of carbon dioxide sequestration in brine. Nottingham:; 2012.

42. Merkel BJ, Planer-Friedrich B. Groundwater Geochemistry: A Practical Guide to Modelling of Natural and Contaminated Aquatic Systems Berlin: Springer; 2008.

43. HYDRAFACT. HydraFLASH HYDRATE & PREDICTION SOFTWARE. [Online].; 2015 [cited 2015 March 10. Available from: http://www.hydrafact.com/index.php?page=software.

44. PennState Department of Energy and Mineral Engineering. Soave-Redlich-Kwong EOS (1972). [Online].; 2014 [cited 2015 March 10. Available from: https://www.e-education.psu.edu/png520/m10_p5.html.

45. PennState Department of Energy and Mineral Engineering. Peng-Robinson EOS (1976). [Online].; 2014 [cited 2015 March 10. Available from: https://www.e-education.psu.edu/png520/m11_p2.html.

46. Masoudi R, Arjmandi M, Tohidi B. Extension of Valderrama–Patel–Teja equation of state to modelling single and mixed electrolyte solutions. Chemical Engineering Science. 2003 May; 58(9).

47. Diamantonis NI, Boulougouris GC, Mansoor E, Tsangaris DM, Economou IG. Evaluation of Cubic, SAFT, and PC-SAFT Equations of State for the Vapor-Liquid Equilibrium Modeling of CO2 Mixtures with Other Gases. Industrial & Engineering Chemistry Research. 2013 February; 52(10).

48. Kontogeorgis GM, Yakoumis IV, Vlamos PM. Application of the sCPA equation of state for polymer solutions. Computational and Theorectical Polymer Science. 2000 August; 10(6).

49. Manning CE, Aranovich LY. Brines at high pressure and temperature: Thermodynamic, petrologic and geochemical effects. Precambrian Research. 2014 July; 253.

50. Duan Z, Moller N, Weare JH. An equation of state for the CH4-CO2-H20 system: I. Pure systems for 0 to 1000C and 0 to 8000 bar. Geochimica et Cosmochimica Acta. 1992; 56.

51. Gross J, Sadowski G. Application of the Perturbed-Chain SAFT Equation of State to Associating Systems. Industrial & Engineering Chemistry Research. 2002 October ; 41(22).

52. Gross J, Sadowski G. Perturbed-Chain SAFT: An Equation of State Based on a Perturbation Theory for Chain Molecules. Industrial & Engineering Chemistry Research. 2001 January ; 40(4).